

ARTICLE OPEN

Biosorption removal of iron from water by *Aspergillus niger*M. M. Zareh¹✉, Ashraf S. El-Sayed² and Dina M. El-Hady¹

The expulsion of iron from water is an essential issue. Exceeding iron concentrations in water, it become more toxic and cause several troubles for human health and environment. The biosorption is the upcoming mechanism to treat the iron from wastewater. Microorganisms perform an important function in the bioremediation of wastewater. This study was conducted to investigate the removal of iron by dried biomass of *Aspergillus niger* (*A.niger*). The dried *A. niger* was tested as a sorbent for the removal of iron from wastewater. The effects of various experimental parameters as initial iron concentration, amount of biomass, contact time and the initial pH solution were examined and optimal experimental conditions were obtained. The obtained adsorption results were fitted to the Langmuir, Freundlich, and Temkin equations. The study showed that dried *A. Niger* biomass in high concentration 4 g/100 ml was found to be more effective in the removal of iron from water at pH 3 with contact time 60 min. the *A. Niger* successfully removed iron and has ability to be regenerated and reused in the removal process.

npj Clean Water (2022)5:58; <https://doi.org/10.1038/s41545-022-00201-1>

INTRODUCTION

Water is life. By this sentence, we can describe the importance of water for almost every living creature. As it is known that human can live without solid food for about 20 days, but without water human begins battling for life after 1 day. Iron is one of the essential elements for human life or environment in trace concentration. The daily requirement of iron according to Prashant et al. is in range 1–2 mg/day of which 75% are found in the blood and the rest 25% are in the bone marrow and liver¹. Iron has biochemically accessible valence status that plays a role in a wide variety of electron transfer processes and enzymatic activities². The presence of iron in water plays an important role as it enhances the growth of iron reducing bacteria that aid in the conversion of iron (II) to iron (III) via oxidation³. However, its high values cause several health problems such as anorexia, diarrhea, diphasic shock, metabolic acidosis, vascular congestion of the gastrointestinal tract, brain, spleen and thymus, and death at overdose⁴.

In the environment, iron exists in two forms, which are soluble ferrous iron and insoluble ferric particulate iron⁴. It is commonly found in natural fresh water, but its concentration different according to geographical location. Joe-Wong et al.⁵ reported that the geology of environment is the main factor controlling groundwater hydrology. In addition, iron is found in rocks and soil. Under proper conditions, iron will leach into the water resources from rock and soil formations. So, the contamination of iron (Fe) in groundwater occurs naturally or by anthropogenic sources including industrial effluent, landfill leakage and acid mine drainage. Well casings, pump components, pipes and storage tanks can also contribute to Fe ion water contamination^{4,6}.

Water containing high doses of iron (Fe⁺³) can stain clothes, dishware, discolor plumbing fixtures, and sometimes add a rusty look and tasty to the water⁷. Exceeding iron (Fe⁺³) concentrations produce a yellow to reddish appearance in water. When the concentration of iron in water is very high, it become more toxic and cause several troubles for human health. Hence, iron must be uptake or transformed to less toxic form in water before using in irrigation or before being discharged to the environment. There are no health-based guidelines for the concentration of iron in

drinking water standard for all the world. However, based on taste and nuisance considerations the permissible limit for iron in drinking water is (0.3 mg/l) according to the world health organization (WHO) and environment protection agency (EPA)⁸.

Increased urbanization and industrialization activities such as electroplating, steel manufacturing, wood preservation, tanning and glass manufacturing lead to increase the heavy metals and other pollutants into the water and environment^{9–17}. Water pollution occurred by changes in physical, chemical and biological parameters of water that has a dangerous impact on environment and human health^{18–20}. The presence of these heavy metals in environment and water exposure the human to many serious diseases including autoimmune disorder, digestive disorder, heart disorder, liver, kidney, stomach and lung cancer^{21–27}. The expulsion of heavy metal such as iron from water is an essential issue. At present various distinctive mechanisms are used for removal or decreasing the amounts of heavy metals for examples, ion exchange, coagulation, chemical precipitation, solvent extraction, adsorption and membrane separation. These mechanisms have some disadvantages such as incomplete removal, generation of toxic sludge and high cost specially in lower concentration of heavy metals^{28–30}.

Biosorption is the upcoming mechanism to treat the heavy metal such as iron (Fe⁺³ ions) from wastewater by metabolizing it or by using physico-chemical mechanism. Different microorganism like algae, bacteria, yeast, and fungi have shown the capability biosorption of iron (Fe⁺³ ions) besides it is highly efficient, economic, and environmental^{2,3,31–39}. The biosorption process depend on different factors as the types of metal ions, the cell wall structure of biomass, pH, contact time with biomass, and metal concentration^{30,40,41}.

Several studies have shown the capability of *A. niger* to treat heavy metals from aqueous solutions. Some studies have proved the removal of zinc (Zn), cobalt (Co), cadmium (Cd), lead (Pd), chromium (Cr), copper (Cu), and nickel (Ni)^{42–49}.

The aim of the present study was to investigate the ability of *Aspergillus niger* (*A.niger*), for the removal of iron from wastewater. The study was concentrated on the adsorption property as one of the physicochemical properties of *A. niger* fungi. Ferric and ferrous are the most common soluble iron forms. Ferric is a more stable

¹Department of Chemistry, Faculty of Science, Zagazig University, Zagazig 44519, Egypt. ²Enzymology & Fungal Biotechnology Lab, Botany & Microbiology Department, Faculty of Science, Zagazig University, Zagazig 44519, Egypt. ✉email: mmzareh@zu.edu.eg

form than ferrous. In addition, ferrous is easily converted to ferric. Accordingly, it is better to perform the study on ferric iron rather than ferrous. Furthermore, the purpose was to study the efficiency of bioremoval of iron (Fe^{+3} ions) from aqueous solution by *A. niger* under different conditions of adsorbent dosage, initial concentration, pH and contact time. Additionally, the biosorption kinetics, equilibrium and Langmuir, Freundlich, and Tamkin isotherms were analyzed. Also, the nature of biosorption of iron was studied.

RESULTS AND DISCUSSION

Effect of fungal powder biomass weights on Fe^{+3} removal

The effect of fungal powder biomass weights on Fe^{+3} removal was examined for (0.5, 1, 1.5, 2, 2.5, 3, 3.5, 4, and 5 g) for *A. niger*. Figure 1 shows that the percent of Fe^{+3} removal by *A. niger* increased by increasing the initial biomass weights till reaching the high value (86.56%) at 4 g. Then, it was slightly increasing to the highest removal percent (88.17%). The reason for this increase explained in accordance with Mondal's study and Siwi's study attributed to an increase in area of the absorptive surface and the availability of free active binding sites on the surface of biomass^{47,50}. Therefore, this observation indicates that the optimum level of fungal powder biomass weight that should be used in the following experiments was 4 g/100 ml in the case of *A. niger*.

Effect of contact time on Fe^{+3} ion removal

The effect of contact time on Fe^{+3} removal by fungal biomass was examined at (30, 60, 90, and 120 min) for *A. niger*. Figure 2 shows that the percent of Fe^{+3} removal by *A. niger* increased by increasing the contact time till reaching the maximum at 60 min (86.56%). Then, it decreased by increasing the contact time more than 60 min.

According to the obtained results, it was observed that the removal of iron increased with increasing the amount of *A. niger* in aqueous solution till reach maximum and then decreased. This is like the previous studies which reported that by passing the time

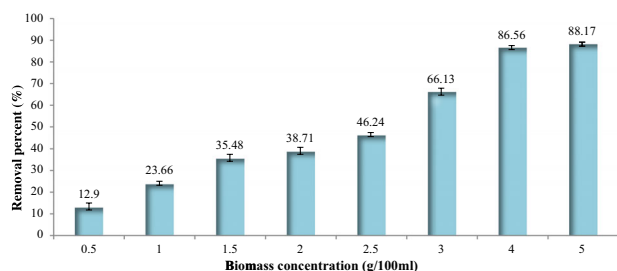


Fig. 1 Effect of variation of the weight of *A. niger* bioadsorbent on the removal percent of iron III, when using (0.01 M) Fe^{+3} as initial solution at the solution pH 2.4 and for a contact time 60 min at room temperature. $n = 3$ determinations.

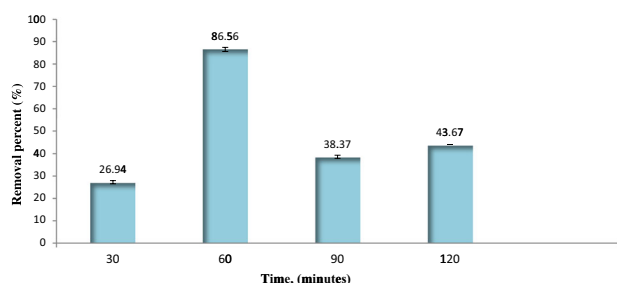
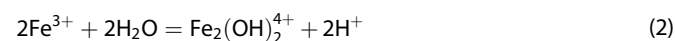
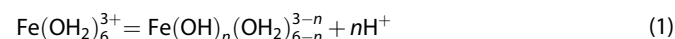


Fig. 2 Effect of contact time on the removal percent of iron III when the initial concentration was (10^{-2} M), at solution pH 2.4, and using 4 g/100 ml of *A. niger* as bioadsorbent at room temperature. $n = 3$ determinations.

the free binding active sites in the outer surface were saturated³⁵. Therefore, the adsorption process happened in the outer surface instead of the inner surface. Due to the smaller inner surface area, the increased contact time causes efficiency to decrease. This result in accordance to Darama's study, who reported that the biosorption of zinc ions increased by increasing time contact till reached equilibrium time then decreased⁵¹.

After longer time (90 min and above) another factor can affect the adsorption process is the hydrolysis of the non-adsorbed free Fe^{3+} with time leading to the formation of $\text{Fe}(\text{OH})_2^+$, $\text{Fe}(\text{OH})_2^{2+}$ and $\text{Fe}(\text{OH})_3$ which decreases the probability of the biosorption³⁵. These compounds are likely to be formed and cannot be associated with the amine group of the biomass. This equilibrium⁵² releases H^+ as shown below. This was reported for Fe^{3+} concentrations $>10^{-3}$ M.



In this study 10^{-2} M solution was subjected for evaluating the effect of contact time. Due to the smaller size of the liberated H^+ than Fe^{3+} ions, their competition could be a reason of the desorption that occur after time longer than the equilibrium value (60 min).

Effect of initial Fe^{+3} concentration on Fe^{+3} removal

The effect of initial Fe^{+3} concentration on Fe^{+3} removal by the fungal biomass was examined for (481.19, 32.55, 9.44 and 0.205 mg/100 ml) for *A. niger*. Figure 3 shows that the amount of Fe^{+3} removal by *A. niger* increased by increasing the initial Fe^{+3} concentration till reaching the maximum at 9.44 mg/100 ml (88.01%). Then, it decreased by increasing the initial Fe^{+3} concentration.

These results were explained due to the proportion of the free active binding sites compared to the initial number of Fe^{+3} ions in the lower concentration are more, thereby tending to an increase in biosorption process. In the higher concentration these sites become less and occupied, thereby tending to a decrease in biosorption process. The results of the present study agreed with several previous studies^{2,34,36,53,54}.

Effect of initial pH values of solution on Fe^{+3} removal

The effect of initial pH on Fe^{+3} removal was examined by varying the pH value (2.5, 3, 3.5, and 4). From this study, the pH value suitable for the best removal percentage was found. Figure 4 shows that the optimum pH value for *A. niger* was 3, where the Fe^{+3} -removal percent was highest (96.34%). At pH value 2.5, the Fe^{+3} -removal percent was only 86.56%. At this value (pH 3), ferric ions were easily converted to ferric hydroxide that helped Fe^{+3} removal⁵⁵.

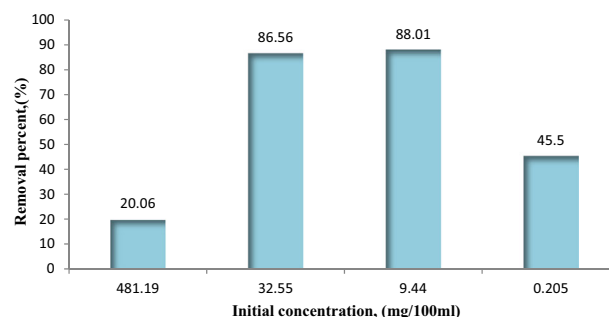


Fig. 3 Effect of initial Fe^{+3} concentration (0.203–481.19 mg/100 mL) on the removal percentage of iron III by using 4 g/100 ml of *A. niger* as bioadsorbent at the solution pH 2.4 at room temperature and for a contact time 60 min. $n = 3$ determinations.

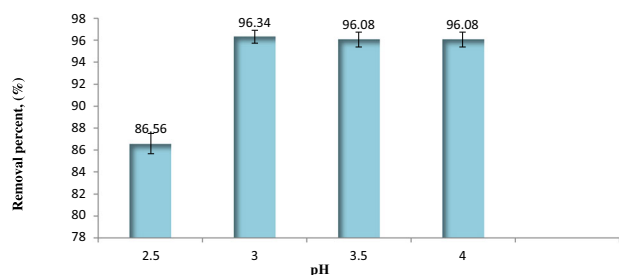


Fig. 4 Effect of pH on the removal percent of iron III by using *A. niger* as bioadsorbent when the initial concentration was (10^{-2} M) using 4 g/100 ml of the biomass at room temperature and for 60 min time contact. $n = 3$ determinations.

Effect of presence of NaCl as inert salt on Fe^{+3} removal and regeneration of biomass

The presence of NaCl as inert salt enhanced the percent of Fe^{3+} removal by (7.57%) than in absence of NaCl.

Regeneration of the used biomass is of importance for recycling purposes. 0.1 N HCl was applied for the regeneration for fungal biomass. It worked like a desorbing agent that removes the binded ferric ions. In case of *A. niger* the percent of Fe^{+3} removal decreased from 88.01% to 31.86%. Xiao's study explained this because of the competitive effect of the remained free H^+ ions⁵⁶. In spite of the Fe^{+3} desorbed biomass was washed several times with double distilled water till the washed solution pH reaching neutral, the remained free H^+ ions on the fungal biomass surface compete with the vacant sites binding. Therefore, the Fe^{+3} removal decreased because of the decrease in the available free binding sites on the adsorbent fungal biomass. Jaafarzadeh⁵⁷ reported that the biosorption capacity of cadmium decreased after desorbed by 1 M of hydrochloric acid.

The reloading capacity = amount of Fe^{+3} removal in the second cycle/amount of Fe^{+3} removal in the first cycle 0.362.

Isotherm models of biosorption

The adsorption isotherm models were evaluated for iron at the solution pH and contact time of 60 min with 4 g of *A. niger*. The obtained result could fit the Langmuir⁵⁸, Freundlich⁵⁹ and Temkin⁶⁰ isotherms models by ignoring the extremely low value of Fe^{+3} concentration.

The isotherms constants were calculated to find out the adsorption capacity of the *A. niger* for Fe^{+3} . The values of isothermal constants (K_a , K_f , and b_T) and correlation coefficients R^2 are shown in Table 1 for Langmuir, Freundlich, and Temkin models.

That results indicated that the biosorption data was best fitted in Temkin as compared to Langmuir and Freundlich models. The Langmuir constant (K_a) and Freundlich constants (K_f and n) values were determined from slope and intercept of the plot.

Langmuir isotherm was charted between $1/q_e$ and $1/C_e$ as shown in Fig. 5.

The Langmuir model assumes that the maximum amount of Fe^{+3} adsorbate on the homogenous surface of fungal biomass (biosorbent) take place in saturated monolayer form. The monolayer saturation capacities, q_{max} is 29.41 mg/g for *A. niger*. The values of R_L were 0.9864, 0.6126, 0.3144, and 0.0301 for the initial Fe^{+3} concentrations 2.051, 94.39, 325.46, and 4811.98. The R_L values indicate that sorption was more favorable for the lower initial metal ion concentrations than for the higher ones.

Freundlich isotherm was charted between $\log q_e$ and $\log C_e$ as shown in Fig. 6.

Temkin isotherm was charted between q_e and $\ln C_e$ as shown in Fig. 7.

The conclusions from the present study, fungi is that the powder biosorbent of *A. niger* was applied successfully for the sorption of

Table 1. Parameters of Langmuir, Freundlich, and Temkin isotherms for the biosorption of Fe^{+3} by *A. niger*.

Langmuir isotherm model		
q_{max}	k_a	R^2
29.41	0.0067	0.9991
Freundlich isotherm model		
n	k_f	R^2
2.604	1.107	0.9139
Temkin isotherm model		
A_T	b_T	
0.1499	653.368	
B	R^2	
3.792	0.9999	

iron metal from wastewater. The biosorption process was dependent on the amount of biomass, the contact time, the initial concentration of iron in water and the initial pH of solution. Biosorption increased rapidly by increasing the amount of biomass till reaching maximum then it slightly increased. While the biosorption increased by increased the contact time and concentration of iron till reach maximum then decreased. The lower pH enhanced the efficiency of biosorption process as it prevents the ferric ions converted to the ferric hydroxide precipitation so the percent of Fe^{+3} removal could be measured accurately. The sorption data fitted into Langmuir, Freundlich, and Temkin isotherms models. The obtained Temkin isotherm model showed more fitting than Langmuir and Freundlich models due to the highest regression.

METHODS

Reagents and materials

Potato dextrose medium (PDA), Ferric Nitrate ($\text{Fe}(\text{NO}_3)_3 \cdot 9\text{H}_2\text{O}$, assay 99%) [Alpha Chemika, India], EDTA (assay 99%) [Adwic, Cairo], Magnesium Sulfate (MgSO_4 , assay 98%) [Adwic, Cairo], Ammonium Chloride (NH_4Cl , assay 99%) [Adwic, Cairo], Ammonia Solution (assay 33%) [Adwic, Cairo], Sodium Acetate Anhydrous (NaCH_3COO , assay 99%) [Adwic, Cairo], Acetic Acid (glacial assay 98%) [Alpha Chemicals, Cairo], Salicylic Acid (assay 99%) [Adwic, Cairo], Acetone (assay 99%) [Adwic, Cairo], Hydrochloric Acid (HCl, assay 30–34%) [Research lab, India], Sodium Hydroxide (NaOH, assay 98%) [Alpha Chemicals, Cairo] and bi-distilled water was used for preparation and dilution of all the prepared solutions.

Equipment

Atomic Adsorption Spectrophotometer (AAS) [model 969 AA Spectrometer, Unicam, 1999] and pH meter.

Preparation of fungal biomass

A. niger was isolated from plants "endophytic fungi" from ficus elastic⁶¹. This fungal isolate was morphologically and molecular identified⁶² and stored as fungal stock culture as slope culture at 4 °C.

Potato dextrose medium (PDA) was used for the growth of *A. niger*⁶³. The slants were incubated for 7 days at 30 °C. The cultures were maintained at 4 °C and subculture every 14 days. A plug (4-mm diameter, equal 2×10^7 spore) was inoculated into a sterilized

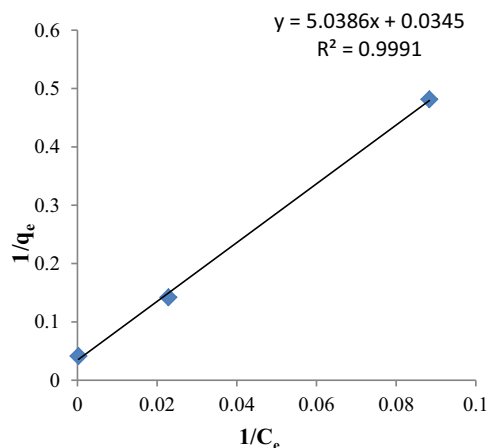


Fig. 5 Langmuir adsorption isotherm of Fe^{+3} in case of *A. niger* as biomass. The isotherm was measured for initial values of iron (III) between 2.052 and 4811.98 mg/L, at room temperature, at optimum condition for the best adsorption (pH = 2.4, time of adsorption 60 min and for 4 g biomass).

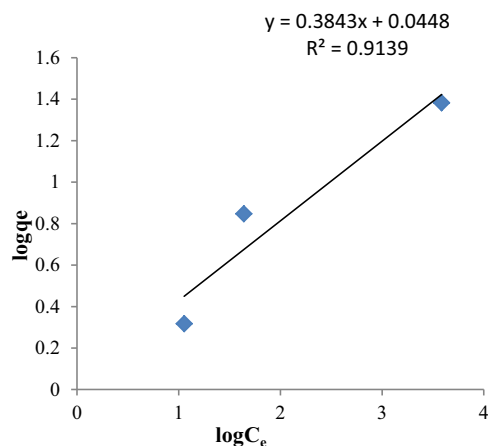


Fig. 6 Freundlich adsorption isotherm of Fe^{+3} in case of *A. niger* as biomass. The isotherm was measured for initial values of iron (III) between 2.052 and 4811.98 mg/L, at room temperature, at optimum condition for the best adsorption (pH = 2.4, time of adsorption 60 min and for 4 g biomass).

potato dextrose broth (PDB) medium. The flasks were incubated for 14 days at 30 °C. At the end of incubation period, the fungal biomass was filtrated by filter paper, washed several times with distilled water, and dried in oven at 55 °C for 24 h and ground with a mortar to make powder biomass.

Preparation of Fe^{+3} solution and the solution standardize

The stock solution of Fe^{+3} ions (0.1 M) was prepared by dissolving 10.1 g of $\text{Fe}(\text{NO}_3)_3 \cdot 9\text{H}_2\text{O}$ in 250 ml of distilled water. Other concentrations were prepared from the stock solution by dilution varied between (10^{-2} , 10^{-3} , and 10^{-4}). The stock Fe^{3+} solution was standardized against EDTANa_2 standard solution using salicylic acid indicator, which was validated according to ICH^{64,65}.

Analytical methods

The amount of Fe^{+3} before and after the adsorption were determined by either titration against EDTA or atomic absorption

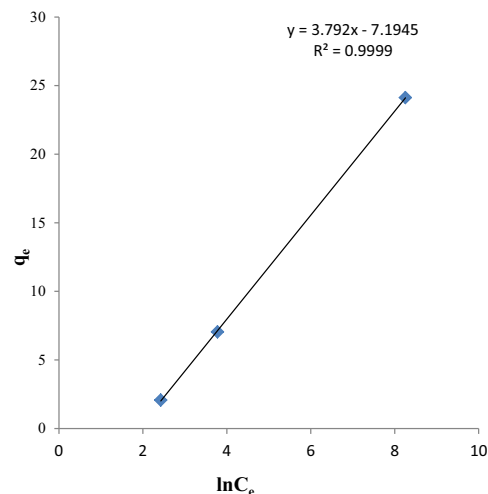


Fig. 7 Temkin adsorption isotherm of Fe^{+3} in case of *A. niger* as biomass. The isotherm was measured for initial values of iron (III) between 2.052 and 4811.98 mg/L, at room temperature, at optimum condition for the best adsorption (pH = 2.4, time of adsorption 60 min and for 4 g biomass).

spectrophotometer analysis. Then, the results are compared to each other.

The removal percent were calculated³⁵ by using the following equation

$$\text{Removal percent (\%)} = ((C_i - C_e)/C_i) * 100 \quad (3)$$

where C_i is the initial concentration of Fe^{3+} and C_e is the equilibrium concentration of Fe^{3+} after adsorption.

Several powder biomass weights (0.5, 1, 1.5, 2, 2.5, 3, 3.5, 4, and 5 g) for *A. Niger* were tried³⁵. The Fe^{+3} removal was studied by addition of the weighed amount of the powder biomass to 100 ml of (10^{-2} M) of Fe^{+3} solution and shaken for 60 min. Then, the percent of Fe^{+3} removal was calculated as indicated before.

The effect of contact time³⁵ on efficiency of Fe^{+3} removal was studied. Different time intervals (30, 60, 90, and 120 min) for *A. niger* were tried. The Fe^{+3} removal was studied by addition of 4 g of *A. niger* to 100 ml of (10^{-2} M) of Fe^{+3} solution and shaken. Then, the percent of Fe^{+3} removal was calculated as indicated before.

The effect of varied initial Fe^{+3} concentrations on efficiency of Fe^{+3} removal was studied. Different initial Fe^{+3} concentrations (481.19, 32.55, 9.44 and 0.205 mg/100 ml) for *A. niger* were tried. The Fe^{+3} removal was studied by addition of 4 g of *A. Niger* to 100 ml of Fe^{+3} solution and shaken for 60 min. Then, the percent of Fe^{+3} removal was calculated as indicated before.

The effect of initial pH value was studied. Different initial pH values (2.5, 3, 3.5, and 4) were tried. The Fe^{+3} removal was studied by adjusting the pH of 100 ml of (10^{-2} M) of Fe^{+3} solution by using 0.1 N NaOH. Then, added 4 g of *A. Niger* to 100 ml of Fe^{+3} solution and shaken for 60 min for *A. Niger*. Then, the percent of Fe^{+3} removal was calculated as indicated before.

The effect of addition of 0.4 g of NaCl (assay 99.5%) to 100 ml of (10^{-3} M) of Fe^{+3} solution was studied. The Fe^{+3} removal was estimated for optimum fungal dry weight 4 g of *A. Niger*. The mixture was shaken for 60 min at the solution pH. Then, the percent of Fe^{+3} removal was calculated as indicated before.

Regeneration of biomass

The biomass obtained after the desorption process was washed with (0.1 N) hydrochloric acid (assay 30–34%). Then, it was thoroughly washed several times by bi-distilled water to get the neutral pH of washed solution. Then, they were dried and

re-suspended in 100 ml of (10^{-3} M) of Fe^{+3} solution and shaken for 60 min at the solution pH. The reloading capacity was calculated as following equation:

The reloading capacity = amount of Fe^{+3} removal in the second cycle/amount of Fe^{+3} removal in the first cycle.

Isotherm models of biosorption

Iron biosorption was analyzed using Langmuir, Freundlich, and Temkin isotherms models to study the adsorption behavior to investigate the performance of the biosorption process under different operating conditions. The adsorption isotherm models were applied at different induced Fe^{+3} concentrations.

The amount of Fe^{+3} removal on the fungal biomass q (mg/g) was calculated according to the following equation:

$$q = (C_i - C_e)V/W \quad (4)$$

where C_i is the initial concentration of Fe^{+3} ions before adding fungal biomass (mg/l), C_e is the equilibrium concentration of Fe^{+3} ions after adding fungal biomass (mg/l), V is the volume taken from Fe^{+3} ions solution (l) and W is the amount of fungal biomass taken (g).

The Langmuir⁵⁸ adsorption isotherm is utilized to describe chemisorption process when the adsorbent and the adsorbate formed ionic or covalent chemical bonds. This model can be written in linear form:

$$1/q_e = 1/q_{\max} + \left(1/q_{\max} k_a\right)(1/C_e) \quad (5)$$

where q_e is the equilibrium amount of adsorbate on fungal biomass (mg/g), q_{\max} is the maximum amount of adsorbate on fungal biomass (mg/g) and k_a is the Langmuir constant (the maximum adsorption capacity in mg/l).

The magnitude of a dimensionless constant R_L was used to determine the quality of Langmuir adsorption isotherm (the separation factor) can be calculated by the following equation:

$$R_L = 1/(1 + C_0 k_a) \quad (6)$$

The parameter R_L indicates the shape of the isotherm accordingly:

Value of R_L Type of isotherm

$0 < R_L < 1$ Favorable

$R_L > 1$ Unfavorable

$R_L = 1$ Linear

$R_L = 0$ Irreversible

The empirical Freundlich adsorption isotherm is utilized to describe adsorption on a heterogenous surface⁵⁹. This model can be written in linear form:

$$\log q_e = \log k_f + 1/n (\log C_e) \quad (7)$$

where k_f is the Freundlich constant (the adsorbent capacity in mg/g) and n is the Freundlich coefficient (the adsorbent intensity in mg/l).

The Temkin isotherm contains the factor that taking into the account of adsorbent–adsorbate interactions⁶⁰. That is utilized to describe the assumption that a fall in the heat of sorption is linear rather than logarithmic, as shown in Freundlich isotherm. This model can be written in linear form:

$$q_e = B \ln A_T + B \ln C_e \quad (8)$$

$$B = [RT/b_T] \quad (9)$$

where A_T is Temkin isotherm equilibrium constant (l/g), B is constant related to heat of sorption (J/mol), R is universal gas constant (8.214 J/mol/K), T is temperature at 298 K, and b_T is Temkin isotherm constant.

DATA AVAILABILITY

All data generated or analyzed during this study are included in this published article.

CODE AVAILABILITY

Code is available from the corresponding author upon reasonable request.

Received: 8 March 2022; Accepted: 4 October 2022;

Published online: 01 November 2022

REFERENCES

- Prashanth, L., Kattapagari, K. K., Chitturi, R. T., Baddam, V. R. R. & Prasad, L. K. A review on role of essential trace elements in health and disease. *J. Dr. NTR Univ. Health Sci.* **4**, 75–85 (2015).
- Bourzama, G. et al. Iron uptake by fungi isolated from Arcelor Mittal -Annaba- in the Northeast of Algeria. *Braz. J. Poultry Sci.* <https://doi.org/10.1590/1806-9061-2020-1321> (2021).
- WHO. Guidelines for drinking-water quality: fourth edition incorporating the first addendum. <https://www.who.int/publications/i/item/9789241549950> (2017).
- Marsidi, N., Abu Hasan, H. & Abdullah, S. A review of biological aerated filters for iron and manganese ions removal in water treatment. *J. Water Process Eng.* **23**, 1–12 (2018).
- Joe-Wong, C., Brown, G. E. & Maher, K. Kinetics and products of chromium (VI) reduction by iron (II/III)-bearing clay minerals. *Environ. Sci. Technol.* **51**, 9817–9825 (2017).
- Ajiboye, T. O., Oyewo, O. A. & Onwuodi, D. C. Simultaneous removal of organics and heavy metals from industrial wastewater: a review. *Chemosphere* **262**, 128379 (2019).
- Dueik, V., Chen, B. K. & Diosady, L. L. Iron-polyphenol interaction reduces iron bioavailability in fortified tea: competing complexation to ensure iron bioavailability. *J. Food Qual.* **2017**, 1–7 (2017).
- The Environmental Protection Agency (EPA). Drinking water regulations and contaminants. <https://www.epa.gov/dwregdev/drinking-water-regulations-and-contaminants#List> (2019).
- Brusseau, M., Pepper, I. & Gerba, C. *Environmental and Pollution Science* (Academic Press, 2019).
- Cao, W., Wang, Z., Ao, H. & Yuan, B. Removal of Cr(VI) by corn stalk based anion exchanger: the extent and rate of Cr(VI) reduction as side reaction. *Colloids Surf. A Physicochem. Eng. Asp.* **539**, 424–432 (2018).
- El-Beltagi, H. S., Sofy, M. R., Aldaej, M. I. & Mohamed, H. I. Silicon alleviates copper toxicity in flax plants by up-regulating antioxidant defense and secondary metabolites and decreasing oxidative damage. *Sustainability* **12**, 4732 (2020).
- Olawale, S. A. Biosorption of heavy metals from aqueous solutions: an insight and review. *Arch. Ind. Eng.* **3**, 1–31 (2021).
- Qasem, N. A. A., Mohammed, R. H. & Lawal, D. U. Removal of heavy metal ions from wastewater: a comprehensive and critical review. *npj Clean Water* **4**, 36 (2021).
- Su, P., Zhang, J., Tang, J. & Zhang, C. Preparation of nitric acid modified powder activated carbon to remove trace amount of Ni(II) in aqueous solution. *Water Sci. Technol.* **80**, 86–97 (2019).
- Wang, J. et al. Biosorption of hexavalent chromium from aqueous solution by polyethyleneimine-modified ultrasonic-assisted acid hydrochar from Sargassum horneri. *Water Sci. Technol.* **81**, 1114–1129 (2020).
- Zglobicki, W. Special issue on heavy metals in the environment—causes and consequences. *Appl. Sci.* **12**, 835 (2022).
- Zhang, Y. & Duan, X. Chemical precipitation of heavy metals from wastewater by using the synthetic magnesium hydroxy carbonate. *Water Sci. Technol.* **81**, 1130–1136 (2020).
- Rajeshkumar, S. et al. Studies on seasonal pollution of heavy metals in water, sediment, fish and oyster from the Meiliang Bay of Taihu Lake in China. *Chemosphere* **191**, 626–638 (2018).
- Schneider, L. et al. How significant is atmospheric metal contamination from mining activity adjacent to the Tasmanian Wilderness World Heritage Area? A spatial analysis of metal concentrations using airtrajectory models. *Sci. Total Environ.* **656**, 250–260 (2019).
- Su, L., Nan, B., Craig, N. J. & Pettigrove, V. Temporal and spatial variations of microplastics in roadside dust from rural and urban Victoria, Australia: implications for diffuse pollution. *Chemosphere* **252**, 126567 (2020).
- Azimi, A., Azari, A., Rezakazemi, M. & Ansarpour, M. Removal of heavy metals from industrial wastewaters: a review. *ChemBioEng Rev.* **4**, 37e59 (2017).
- Bolisetty, S., Peydayesh, M. & Mezzenga, R. Sustainable technologies for water purification from heavy metals: review and analysis. *Chem. Soc. Rev.* **48**, 463–487 (2019).

23. Fierro, P., Tapia, J., Bertrán, C., Acuña, C. & Vargas-Chacoff, L. Assessment of heavy metal contamination in two edible fish species and water from North Patagonia Estuary. *Appl. Sci.* **11**, 2492 (2021).
24. Huang, Y. et al. Current status of agricultural soil pollution by heavy metals in China: a meta-analysis. *Sci. Total Environ.* **651**, 3034–3042 (2019).
25. Jia, Z., Li, S. & Wang, L. Assessment of soil heavy metals for eco-environment and human health in a rapidly urbanization area of the upper Yangtze Basin. *Sci. Rep.* **8**, 1–14 (2018).
26. Moldovan, A. et al. Spatial variation of water chemistry in Aries River Catchment, Western Romania. *Appl. Sci.* **11**, 6592 (2021).
27. Taseidifar, M., Makavipour, F., Pashley, R. M. & Rahman, A. F. M. M. Removal of heavy metal ions from water using ion flotation. *Environ. Technol. Innov.* **8**, 182–190 (2017).
28. Zglobicki, W. & Telecka, M. Heavy metals in urban street dust: health risk assessment (Lublin City, E Poland). *Appl. Sci.* **11**, 4092 (2021).
29. Renu, N. A., Agarwal, M. & Singh, K. Methodologies for removal of heavy metal ions from wastewater: an overview. *Interdiscip. Environ. Rev.* **18**, 124–142 (2017).
30. Shamim, S. In *Biosorption* (eds. Derco, J. & Vrana B.) Ch. 2 (IntechOpen, 2018).
31. Tran, T.-K., Chiu, K.-F., Lin, C.-Y. & Leu, H.-J. Electrochemical treatment of wastewater: selectivity of the heavy metals removal process. *Int. J. Hydrog. Energy* **42**, 27741–27748 (2017).
32. Díaz-Alarcón, J. A., Alfonso-Pérez, M. P., Vergara-Gómez, I., Díaz-Lagos, M. & Martínez-Ovalle, S. A. Removal of iron and manganese in groundwater through magnetotactic bacteria. *J. Environ. Manag.* **249**, 109381 (2019).
33. Farrag, A. E. H. A. et al. Abu Zenima synthetic zeolite for removing iron and manganese from Assiut governorate groundwater, Egypt. *Appl. Water Sci.* **7**, 3087–3094 (2017).
34. Hassouna, M. E. M. et al. Biosorption of iron by amended *Aspergillus versicolor* from polluted water sources. *Biom. Biostat. Int. J.* **7**, 502–513 (2018).
35. Kalak, T., Dudczak-Halabuda, J., Tachibana, Y. & Cierpiszewski, R. Effective use of elderberry (*Sambucus nigra*) pomace in biosorption processes of Fe(III) ions. *Chemosphere* **246**, 125744 (2020).
36. Krishna Kanamarlapudi, S. L. R. & Muddada, S. Structural changes of *Bacillus subtilis* biomass on biosorption of iron (II) from aqueous solutions: isotherm and kinetic studies. *Pol. J. Microbiol.* **68**, 549–558 (2019).
37. Kulakovskaya, T. et al. The biosorption of cadmium and cobalt and iron ions by yeast *Cryptococcus humicola* at nitrogen starvation. *Folia Microbiol.* **63**, 507–510 (2018).
38. Musah, B. I., Xu, Y., Liang, C. & Peng, L. Biosorption of chromium (VI), iron (II), copper (II), and nickel (II) ions onto alkaline modified *Chlorella vulgaris* and *Spirulina platensis* in binary systems. *Environ. Sci. Pollut. Res. Int.* <https://doi.org/10.1007/s11356-022-19725-7> (2022).
39. Wang, Y. & Huang, K. Biosorption of tungstate onto garlic peel loaded with Fe(III), Ce(III), and Ti(IV). *Environ. Sci. Pollut. Res.* **27**, 33692–33702 (2020).
40. Zada, S. et al. Biosorption of iron ions through microalgae from wastewater and soil: optimization and comparative study. *Chemosphere* **265**, 129172 (2021).
41. El-Naggar, N. E. A., Hamouda, R. A., Mousa, I. E., Abdel-Hamid, M. S. & Rabei, N. H. Biosorption optimization, characterization, immobilization and application of *Gelidium amansii* biomass for complete Pb²⁺ removal from aqueous solutions. *Sci. Rep.* **8**, 13456 (2018).
42. Kim, J.-Y., Oh, S. & Park, Y.-K. Overview of biochar production from preservative-treated wood with detailed analysis of biochar characteristics, heavy metals behaviors, and their ecotoxicity. *J. Hazard Mater.* **384**, 121356 (2020).
43. Acosta-Rodríguez, I., Cárdenas-González, J. F., Rodríguez Pérez, A. S., Oviedo, J. T. & Martínez-Juárez, V. M. Bioremoval of different heavy metals by the resistant fungal strain *Aspergillus niger*. *Bioinorg. Chem. Appl.* **1**, 3457196 (2018).
44. El-Mahdy, O. M., Mohamed, H. I. & Mogazy, A. M. Biosorption effect of *Aspergillus niger* and *Penicillium chrysosporium* for Cd- and Pb-contaminated soil and their physiological effects on *Vicia faba* L. *Environ. Sci. Pollut. Res.* **28**, 67608–67631 (2021).
45. Khan, I. et al. Mycoremediation of heavy metal (Cd and Cr)-polluted soil through indigenous metallotolerant fungal isolates. *Environ. Monit. Assess.* **191**, 585 (2019).
46. Liao, Q. et al. Simultaneous adsorption of As(III), Cd(II) and Pb(II) by hybrid bio-nanocomposites of nano hydroxy ferric phosphate and hydroxy ferric sulfate particles coating on *Aspergillus niger*. *Chemosphere* **223**, 551–559 (2019).
47. Mondal, N. K., Samanta, A., Dutta, S. & Chatteraj, S. Optimization of Cr (VI) biosorption onto *Aspergillus niger* using 3-level Box-Behnken design: equilibrium, kinetic, thermodynamic and regeneration studies. *J. Genet. Eng. Biotechnol.* **15**, 151–160 (2017).
48. Qiu, J. et al. Experimental and modeling studies of competitive Pb (II) and Cd (II) bioaccumulation by *Aspergillus niger*. *Appl. Microbiol. Biotechnol.* **105**, 6477–6488 (2021).
49. Tian, D. et al. A new insight into lead (II) tolerance of environmental fungi based on a study of *Aspergillus niger* and *Penicillium oxalicum*. *Environ. Microbiol.* **21**, 471–479 (2019).
50. Siwi, W. P., Rinanti, A., MDS, S., Hadisoebroto, R. & Fachrul, M. F. Effect of immobilized biosorbents on the heavy metals (Cu²⁺) biosorption with variations of temperature and initial concentration of waste. The 4th International Seminar on Sustainable Urban Development. *IOP Conf. Ser. Earth Environ. Sci.* **106**, 012113 (2018).
51. Darama, S. E. et al. Leaching performance and zinc ions removal from industrial slag leachate using natural and biochar walnut shell. *Environ. Manag.* **67**, 498–505 (2021).
52. Coetzee, R., Dorfling, C. & Bradshaw, S. M. Characterization of precipitate formed during the removal of iron and precious metals from sulphate leach solutions. *J. South. Afr. Min. Metall.* **117**, 771–778 (2017).
53. Xu, H. et al. Removal of lead ions in an aqueous solution by living and modified *Aspergillus niger*. *Water Environ. Res.* **93**, 844–853 (2021).
54. El-Saied, F. A., Abo-Elenan, S. A. & El-shinawy, F. H. Removal of lead and copper ions from polluted aqueous solutions using nanosawdust particles. *Int. J. Waste Resour.* **7**, 305 (2017).
55. Serrano, L. Z., Lara, N. O., Vera, R. R. & Cholico-González, D. Removal of Fe(III), Cd(II), and Zn(II) as hydroxides by precipitation–flotation system. *Sustainability* **13**, 11913 (2021).
56. Xiao, X. et al. Biosorption of cadmium by endophytic fungus (EF) *Microsphaeropsis* sp. LSE10 isolated from cadmium hyperaccumulator *Solanum nigrum* L. *Bioresour. Technol.* **101**, 1668–1674 (2010).
57. Jaafarzadeh, N., Teymouri, P., Babae, A. A., Alavi, N. & Ahmadi, M. Biosorption of cadmium (II) from aqueous solution by NaCl-treated *Ceratophyllum demersum*. *Environ. Eng. Man. J.* **13**, 763–773 (2014).
58. Langmuir, I. The adsorption of gases on plane surfaces of glass, mica and platinum. *J. Am. Chem. Soc.* **40**, 1361–1403 (1918).
59. Freundlich, H. M. F. Over the adsorption in solution. *J. Phys. Chem.* **57**, 385–471 (1906).
60. Temkin, M. & Pyzhev, J. A. V. Kinetics of ammonia synthesis on promoted iron catalysts. *Acta Physicochim.* **12**, 217–222 (1940).
61. El-Sayed, A. S. A. et al. Production, bioprocess optimization and anticancer activity of Camptothecin from *Aspergillus terreus* and *Aspergillus flavus*, endophytes of *Ficus elastica*. *Process. Biochem.* **107**, 59–73 (2021).
62. El-Sayed, A. S. A., Ali, D. M. I., Yassin, M. A., Zayed, R. A. & Ali, G. S. Sterol inhibitor “Fluconazole” enhance the Taxol yield and molecular expression of its encoding genes cluster from *Aspergillus flavipes*. *Process. Biochem.* **76**, 55–67 (2019).
63. Hajahmadi, Z., Younesi, H., Bahramifar, N., Khakpour, H. & Pirzadeh, K. Multi-component isotherm for biosorption of Zn(II), Co(II) and Cd(II) from ternary mixture onto pretreated dried *Aspergillus niger* biomass. *Water Resour. Ind.* **11**, 71–80 (2015). ISSN 2212-3717.
64. Kirakosyan, V. & Davinyan, A. Method validation of compleximetric titration for determination of iron in iron containing drugs. *Der Pharma Chemica* **13**, 57–62 (2021).
65. Zareh, M. M., Saad, M. Z., Hassan, W. S., Elhennawy, M. E., Soltan, M. K. & Sebaiy M. M. (2020) Gradient HPLC Method for Simultaneous Determination of Eight Sartan and Statin Drugs in Their Pure and Dosage Forms. *Pharmaceuticals* **13**, 32. <https://doi.org/10.3390/ph13020032>.

AUTHOR CONTRIBUTIONS

All authors contributed to the study conception and design. Material preparation, data collection and analysis were performed by D.M.El-Hady. as part of her M.Sc. thesis. The first draft of the manuscript was written by D.M.El-Hady, and all authors revised the draft of the manuscript. All authors read and approved the final version of manuscript.

FUNDING

Open access funding provided by The Science, Technology & Innovation Funding Authority (STDF) in cooperation with The Egyptian Knowledge Bank (EKB).

COMPETING INTERESTS

The authors declare no competing interests.

ADDITIONAL INFORMATION

Correspondence and requests for materials should be addressed to M. M. Zareh.

Reprints and permission information is available at <http://www.nature.com/reprints>

Publisher's note Springer Nature remains neutral with regard to jurisdictional claims in published maps and institutional affiliations.



Open Access This article is licensed under a Creative Commons Attribution 4.0 International License, which permits use, sharing, adaptation, distribution and reproduction in any medium or format, as long as you give appropriate credit to the original author(s) and the source, provide a link to the Creative Commons license, and indicate if changes were made. The images or other third party material in this article are included in the article's Creative Commons license, unless indicated otherwise in a credit line to the material. If material is not included in the article's Creative Commons license and your intended use is not permitted by statutory regulation or exceeds the permitted use, you will need to obtain permission directly from the copyright holder. To view a copy of this license, visit <http://creativecommons.org/licenses/by/4.0/>.

© The Author(s) 2022